Denoising PET Images Using Singular Value Thresholding and Stein's Unbiased Risk Estimate*

Ulas Bagci** and Daniel J. Mollura

Center for Infectious Diseases Imaging (CIDI), Department of Radiology and Imaging Sciences, National Institutes of Health (NIH), Bethesda, USA
ulas.bagci@nih.gov

Abstract. Image denoising is an important pre-processing step for accurately quantifying functional morphology and measuring activities of the tissues using PET images. Unlike structural imaging modalities, PET images have two difficulties: (1) the Gaussian noise model does not *necessarily* fit into PET imaging because the exact nature of noise propagation in PET imaging is not well known, and (2) PET images are low resolution; therefore, it is challenging to denoise them while preserving structural information. To address these two difficulties, we introduce a novel methodology for denoising PET images. The proposed method uses the singular value thresholding concept and Stein's unbiased risk estimate to optimize a soft thresholding rule. Results, obtained from 40 MRI-PET images, demonstrate that the proposed algorithm is able to denoise PET images successfully, while still maintaining the quantitative information.

Keywords: PET, Denoising, Singular Value Thresholding, Stein Risk Estimate.

1 Introduction

Positron emission tomography (PET) is a molecular imaging technique that has rapidly emerged as an important functional imaging tool; it provides superior *sensitivity* and *specificity*, when combined with anatomical imaging such as computed tomography (CT) or magnetic resonance imaging (MRI). Since PET has a significantly low number of detected photons, constructed images have high amount of noise (i.e., low signal-to-noise ratio (SNR)). Therefore, there is often a need for denoising PET images to determine accurate quantitative measures for evaluating changes in lesion biology.

Current approaches in PET image denoising are limited to Gaussian smoothing and locally adaptive filtering [1–3]. The majority of researchers focused on

* This research is supported by CIDI, the intramural research program of the National Institute of Allergy and Infectious Diseases (NIAID) and the National Institute of Biomedical Imaging and Bioengineering (NIBIB).

** Corresponding author.

K. Mori et al. (Eds.): MICCAI 2013, Part III, LNCS 8151, pp. 115–122, 2013.

additive Gaussian noise models regardless of the image type, and only a few works have considered characteristics of PET images when developing a denoising technique. In these current approaches, [1–3], one has to carefully chose the spatial width of the Gaussian smoothing filter to yield a good compromise between spatial resolution and SNR. However, smoothing can produce a loss of resolution by averaging voxels together and blurring the distinction between two closely adjacent objects. Moreover, the use of edge preserving or Gaussian smoothing filters are not optimal choices when denoising PET images, unlike the common belief, because PET images are low resolution due to low photon counts and consequential statistical noise. In fact, in PET and other images with *low photon counts* (e.g., SPECT, microscopy), the pixel intensities follow a non-Gaussian distribution. More recently, a Poissonian distribution noise model [4] was suggested to be used in PET images because of the following observations: the noise variance in PET images are **multiplicative**, **asymmetric**, and **varying** over the image [4]. Therefore, it was shown to be feasible to model noise with Poissonian. It is also important to emphasize that the *invariance of the total photon counts* in a PET images or a region of interest (ROI) in PET images should be preserved within some limits so that it does not affect the diagnostic utility of quantification metrics such as standardized uptake value (SUV) which gives physiologically relevant measurements of cellular metabolism.

In [1], locally adaptive filtering (i.e., anisotropic diffusion) was developed to denoise medical images for general purposes; maintaining the edge information, while smoothing the noise was the aim. Although total photon counts were preserved with this approach, the additive noise model, with constant noise variance, violated the non-Gaussian nature of the PET images. In [5], structural information (either from CT or MRI) of matched anatomic images were used in a multi-resolution model to enhance SNR of PET images. However, the presented method is not optimal because one-to-one wavelet parameter exchange between PET images and their anatomical correspondences does not necessarily hold for all subjects. More recently in [2], bilateral filtering was used for denoising PET images. Although improvement in the SNR was observed, substantial change in SUV_{max} was inevitable. To alleviate the challenges described above, we propose to (1) transform PET images with Anscombe's variance stabilizing transform (VST) in order to Gaussianize the image data and inherent noise, (2) remove Gaussianized noise using Stein's unbiased risk estimate and a soft thresholding rule within the popular singular value thresholding (SVT) framework, and (3) apply the inverse variance stabilizing transform (IVST) to obtain denoised PET images. In the next section, we present our proposed framework in detail.

2 Methods

Our approach hinges on the basic notion that medical images are mostly low-ranked due to high correlations of its columns (or rows); therefore, it is possible to model the images with simpler components. For a low-rank matrix, with entries perturbed by Gaussian noise, one may recover an estimate of the low-rank matrix

by using techniques based on the singular value decomposition (SVD). However, accuracy of these estimations are often limited. In practice, since the low-rank matrix is not perturbed by Gaussian noise but rather varying magnitudes–as it is the case in PET images–SVD-based methods are not directly applicable to solve such problems. Herein, we describe a method to Gaussianize PET image noise so that SVD-based methods, SVT in particular, can be applicable. We then apply Stein's unbiased risk estimate formulation to SVT in order to remove noise from the image data.

Anscombe's Variance Stabilizing Transform. Anscombe's VST is a special case of Anscombe's theorem [4], and it allows a Gaussianization of the Poission distribution. According to the theorem, if S is Poission distribution (i.e., $S \sim P(\xi)$ where $\sqrt{\xi}$ is the standard deviation of noise), then there is a function VST such that $\mathbf{Y} = VST(S) = 2\sqrt{S + 3/8}$ when $\xi \to \infty$. Practically, $\mathbf{Y}$ is approximately Gaussian with unit variance for $\xi > 10$ [4], so once the PET images are transformed with Anscombe's VST, Gaussianized noise can be removed with the proposed methodology. Next, an inverse of Anscombe's VST is required to transform denoised PET data back into the SUV domain. IVST of the estimated signal is straightforward as VST is explicit.

Singular Value Thresholding. Assume that a 3-D VST transformed PET image is considered as a stack of slices and each slice is denoted as matrix $\mathbf{Y}$, with a $m \times n$ dimension and the observed PET image is denoted by S. In denoising, we estimate the original data matrix $\mathbf{X}$ from noisy observations: $\mathbf{Y}_{ij} = \mathbf{X}_{ij} + \mathbf{N}_{ij}$, for $i = 1...m, j = 1...n$, where noise $\mathbf{N}$ is modeled as the additive Gaussian, with a constant variance τ: $\mathbf{N} \sim \mathcal{N}(0, \tau^2)$. Since VST is applied to original PET images, the resultant images include residual noise with an approximate constant variance; hence, the Gaussian noise assumption can be used. Conventionally, estimating $\mathbf{X}$ via SVD can simply be done by truncating the singular values of the observed matrix $\mathbf{Y}$, but this truncation mechanism, known as a hard threshold rule, does not provide continuous estimation [6]:

$$SVT_{hard}(\mathbf{Y}) = \underset{\mathbf{X} \in R^{m \times n}}{\operatorname{argmin}} \frac{1}{2}||\mathbf{Y} - \mathbf{X}||_F^2 + \lambda \operatorname{rank}(\mathbf{X}), \tag{1}$$

where λ is a positive scalar, and SVD of the $\mathbf{Y}$ can be defined as $\mathbf{Y} = U\Sigma V^* = \sum_{i=1}^{min(m,n)} \sigma_i u_i v_i^*$. Letting $\mathcal{I}$ be an indicator function denoting the shrinkage of the singular values (i.e., σ_i), then SVT with hard thresholding can simply be written as $SVT_{hard}(\mathbf{Y}) = \sum_{i=1}^{min(m,n)} \mathcal{I}(\sigma_i > \lambda) u_i v_i^*$. Selecting a positive scalar λ is the core of the estimation problem because Eq.1 is minimized when appropriate λ is found. For this type of estimation problem, Stein, in his seminal paper [7], showed that if $\mathbf{Y}_{ij} \sim \mathcal{N}(\mathbf{X}_{ij}, 1)$ with an estimator $\widehat{\mathbf{X}}$ of the form $\widehat{\mathbf{X}} = \mathbf{Y} + g(\mathbf{Y})$, where $g_{ij} \in R^{m \times n} \to R$ is differentiable with respect to $\mathbf{Y}_{ij}$, then the risk of the estimate is given by $E||\widehat{\mathbf{X}} - \mathbf{X}||_F^2 = E\{mn + 2\nabla(g(\mathbf{Y})) + ||g(\mathbf{Y})||_F^2\}$, where ∇ is the first partial derivatives with respect to $\mathbf{Y}_{ij}$. Since mn is constant, choosing a suitable function g that makes $\nabla(g(\mathbf{Y})) + ||g(\mathbf{Y})||_F^2$ everywhere negative will yield

a satisfactory estimate for the problem at hand. However, there is no continuous differentiable function, required by Stein's lemma, in SVT methodology based on hard thresholding rule. In order to avoid a discontinuous estimation caused by the indicator function, one may provide a continuous estimation of λ by shrinking the singular values towards zero, namely called soft thresholding rule for SVT, and it can be formulated as

$$SVT_{soft}(\mathbf{Y}) = \sum_{i=1}^{min(m,n)} (\sigma_i - \lambda)_+ u_i v_i^*. \quad (2)$$

In this equation, since large λ causes a large bias and small λ leads to a high variance, a proper estimation of λ is expected to find the correct trade-off between large bias and high variance in the soft thresholding rule of SVT. As earlier noted, because the soft thresholding rule in SVT formulation (i.e., $(\sigma_i - \lambda)_+$) is continuous, it is differentiable at the singular value matrix (note that derivative of $(\sigma_i - \lambda)_+$ is equivalent to $\mathcal{I}(\sigma_i > \lambda)$ when $\sigma \neq \lambda$) [6]. Hence, SVT_{soft} follows the requirement of the function g stated by the Stein's risk estimation method. Replacing g with SVT_{soft} yields the unbiased risk estimate for SVT as [6]

$$E(SVT_{soft}(\mathbf{Y})) = -mn\tau^2 + \sum_{i=1}^{min(m,n)} min(\lambda^2, \sigma_i^2) + 2\tau^2 \nabla(SVT_{soft}(\mathbf{Y})). \quad (3)$$

The solution of Eq.3 gives the optimum λ such that the risk of the estimate cannot be improved at any point through multiplication of λ by a constant factor. For the computation of the $\nabla(SVT_{soft}(\mathbf{Y}))$ operation, a closed-form expression can be obtained by differentiating $SVT_{soft}(\mathbf{Y})$ with respect to the λ as

$$\nabla(SVT_{soft}(\lambda)) = \sum_{i=1}^{min(m,n)} \left[\mathcal{I}(\sigma_i > \lambda) + |m-n| \left(\frac{\sigma_i - \lambda}{\sigma_i} \right)_+ \right] + 2 \sum_{i \neq j, i, j=1}^{min(m,n)} \frac{\sigma_i (\sigma_i - \lambda)_+}{\sigma_i^2 - \sigma_j^2}. \quad (4)$$

Once λ is found, then denoising is conducted through shrinking singular values of noisy observations $\mathbf{Y}$ towards λ[6]. At the final step, the denoised image is transformed back to the original SUV domain via the Anscombe's $IVST$ method.

3 Experiments and Results

With IRB approval, we collected 40 MRI-PET image sets from 40 different patients. Each patient had either Von-Hippel-Lindau disease, colon cancer, a paraganglioma carcinoid tumor, or hederditary leiomyomatosis renal cell cancer. PET images had a spatial resolution of 4.17 x 4.17 x 2 mm^3. The SNR and

relative contrast of all images were analyzed and compared to other commonly used methods in the literature. The *SUV* analysis–the selected 40 lesions from all the subjects–was conducted to quantify the effect of denoising on the quantitative metrics of PET imaging. For this, we used the SUV_{max} and SUV_{mean} criterion to follow clinical routine. In order to remove any bias towards the proposed method in our evaluations, we transformed PET images via VST prior to conduct experiments for Perona-Malik's, Bilateral, and Gaussian filtering methods so that the noise properties of the transformed PET images were approximately Gaussian. Otherwise, all these approaches diminished the quantitative indexes of PET images considerably.

We first demonstrate the validation of the proposed risk estimate via Monte Carlo estimation. Herein, z independent samples of $\mathbf{Y}$ were drawn from the model of $\mathbf{Y} = \mathbf{X} + \mathbf{N}$. The data matrix $\mathbf{X}$ was constructed based on predefined singular values in low-rank approximation without having repetitive singular values. Then, we computed the average mean squared error between the Stein's unbiased risk estimate and the original matrix by $\frac{1}{z}\sum_{u=1}^{z} ||SVT_{soft}(\mathbf{Y}^u) - \mathbf{X}||_F^2$. Fig. 1a shows the comparison of the risk estimate using Monte Carlo and Stein's unbiased risk estimate for $z = 25$ samples. As clearly seen from the Fig. 1a, Stein's unbiased risk estimate within the SVT framework (solid line), follows the Monte Carlo estimates closely.

Qualitative Evaluation. We qualitatively compared our method with anisotropic diffusion filtering [1], which performed best among the other compared methods. Fig. 1b illustrates the filtered output from the proposed method (ii) and Perona-Malik's method (iii) with respect to the original PET images (i). Red arrows show reduced noise areas in (ii) and limited success of Perona-Malik filtering in (iii) for the corresponding regions. Similarly, the yellow arrows denote the object of interests, where edge information was preserved with the proposed method (ii); however, the object of interests were over-smoothed by the Perona-Malik filtering (iii). As can be seen in all images (rows show different anatomical level of different subjects) in Fig. 1b, the boundary contrast seems to be higher with the proposed method visually, while Perona-Malik's method over-smooths the noisy areas. This is because the proposed method is tuned to preserve fine details of the objects of interests better than Perona-Malik's method.

Quantitative Evaluation. For our quantitative analysis, SNR was used to evaluate the effectiveness of the filtering operation; it is defined as $20 \log 10(\frac{M}{\nu})$, where ν and M indicate the standard deviation and mean of the voxel intensities in a ROI. In order to estimate the SNR levels in the image data, several 3-D ROIs were positioned within the liver and lung areas for all image sets, as it is the convention when measuring SNR in PET images. Positioned ROIs were identical for all filtered and original images. Resulting SNR rates were averaged over all subjects and plotted in Fig. 2a. As it is readily seen, improvement in SNR with respect to the original PET images is higher with the proposed method than the rest. Since a measure of SNR alone may not be sufficient enough to

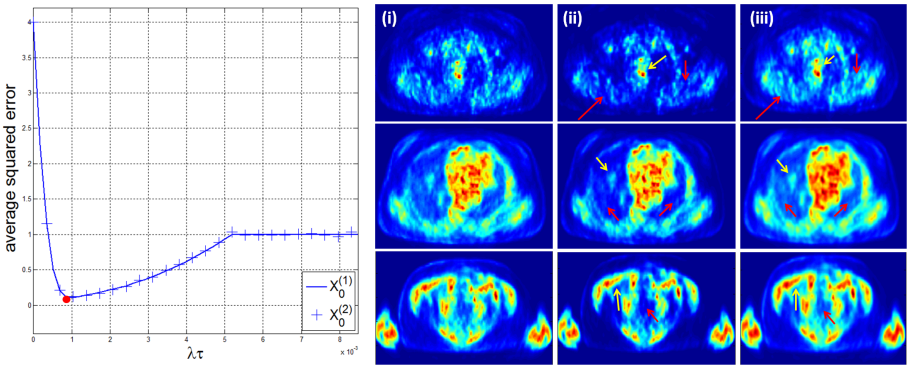

(a) (b)

Fig. 1. (a) $X_0^{(1)}$: Stein's unbiased risk estimate. $X_0^{(2)}$: Monte Carlo estimates. Red point indicates the smallest average squared error (global optima). (b) Each row shows different subjects and different slice levels. (i) Original PET images, (ii) denoised by the proposed method, (iii) denoised by Perona-Malik anisotropic diffusion filtering.

characterize the effectiveness of a filtering method, we also used the concept of *relative contrast* (RC) in our evaluation, where RC was defined as follows [8]:

$$RC = \frac{|M_i^O - M_i^B|}{\sqrt{\nu_i^O \nu_i^B}}, \tag{5}$$

and i implies the specific ROI, M^O and ν^O denote the mean and standard deviation of pixel intensities over the object region O, respectively. Similarly, M^B and σ^B denote the mean and standard deviation of pixel intensities over the background region B, respectively. RC is a measure of object-to-background contrast relative to noise in each region. Object regions were selected from liver and lung areas for each image, as a 3-D ROI, and the resultant RC values are plotted in Fig. 2b. For each experiment, the same set of object and background regions were selected to avoid any bias in the calculations. Note that a higher value of RC indicates a more accurate filtering; hence, the proposed method outperforms all the compared methods, among which Perona-Malik's anisotropic diffusion filtering [1] was having the second higher accuracy due to its property of preserving structural information.

We also investigated how PET specific quantitative markers such as SUV_{max} and SUV_{mean} change after denoising the PET images. For this purpose, 40 lesions from all subjects were identified manually with a fixed ROI, and the quantitative markers were computed for each lesion from (1) the original PET, (2) the filtered image by Perona-Malik's method, and (3) the filtered image by our proposed method. As a comparison, only Perona-Malik's method was used in this evaluation because it was the second best method among other compared methods. The changes of SUV_{max} and SUV_{mean}, for each method and for all

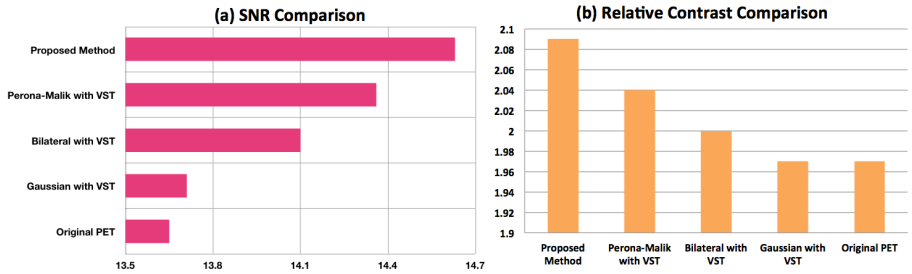

Fig. 2. Proposed method's SNR (a) and *RC* (b) comparison with Perona-Malik's anisotropic filtering, bilateral filtering, and Gaussian smoothing with respect to the original PET images over all subjects are reported

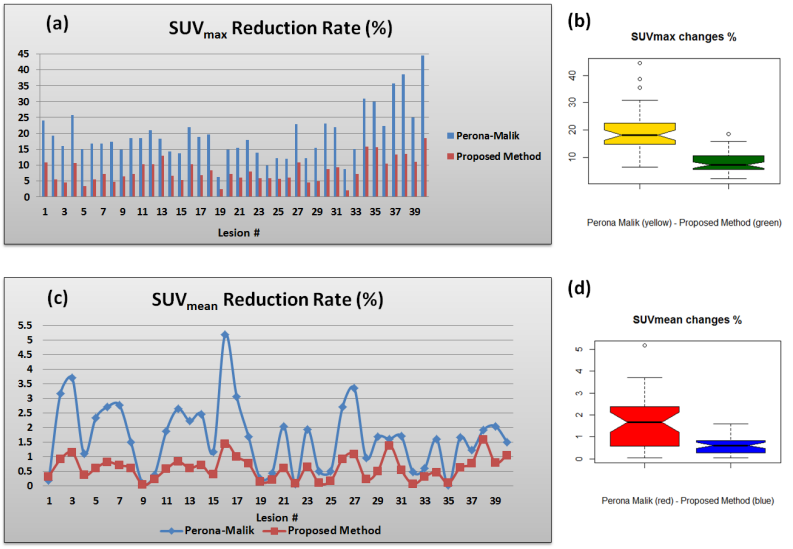

Fig. 3. Comparison of SUV_{max} (a) and SUV_{mean} (c) reduction rates (%) is demonstrated for 40 lesions from different subjects, respectively. Mean (b) and standard deviation (d) of the proposed method and Perona-Malik's filtering is compared through boxplots

lesions, were computed with respect to the original PET images; the comparative results are reported in Fig. 3a and c. In addition, the mean decrease in SUV_{max} and SUV_{mean} values are shown in Fig. 3b and d, respectively. Notice that *smaller changes* in SUV_{max} and SUV_{mean} are highly desirable in order to have a valid denoising method that does not substantially change quantitative markers of the PET imaging. Our experimental results show that when using the proposed method, the reduction rates in SUV_{max} and SUV_{mean} are much smaller than Perona-Malik's method [1].

4 Concluding Remarks

In this study, we presented an effective tool for denosing PET images. The proposed algorithm adapts Stein's unbiased risk estimation within the singular value soft thresholding rule. We also emphasized the usefulness of variance stabilizing transform and its inverse before and after the denoising procedure, respectively, in order to Gaussianiaze the Poissionous nature of the noise in PET images. Experimental results demonstrated that the proposed framework respects the tissue boundaries well, reduces the noise considerably without losing quantitative information of PET images including SUV_{max} and SUV_{mean}. As an extension of this work, we are currently comparing the low-rank data representation algorithms (such as [9]) within the same proposed platform and exploring the model-free algorithms for PET denoising.

References

1. Perona, P., Malik, J.: Scale-space and edge detection using anisotropic diffusion. IEEE Transactions on Pattern Analysis and Machine Intelligence 12(7), 629–639 (1990)
2. Hofheinz, F., Langner, J., Beuthien-Baumann, B., Oehme, L., Steinbach, J., Kotzerke, J., van den Hoff, J.: Suitability of bilateral filtering for edge-preserving noise reduction in pet. EJNMMI Research 1(1), 23 (2011)
3. Turkheimer, F.E., Aston, J., Riddell, C., Cunningham, V.: A linear wavelet filter for parametric imaging with dynamic PET. IEEE Trans. on Medical Imaging 22, 289–301 (2003)
4. Lee, J.A., Geets, X., Gregoire, V., Bol, A.: Edge-preserving filtering of images with low photon counts. IEEE Transactions on Pattern Analysis and Machine Intelligence 30(6), 1014–1027 (2008)
5. Turkheimer, F.E., Boussion, N., Anderson, A.N., Pavese, N., Piccini, P., Visvikis, D.: PET image denoising using a synergistic multiresolution analysis of structural (MRI/CT) and functional datasets. J. Nucl. Med. 49, 657–666 (2008)
6. Candes, E.J., Sing-Long, C.A., Trzasko, J.D.: Unbiased risk estimates for singular value thresholding and spectral estimators. Arxiv (arXiv:1210.4139v1) (2012)
7. Stein, C.M.: Estimation of the mean of a multivariate normal distribution. Annals of Statistics 9(6), 1135–1151 (1981)
8. Saha, P., Udupa, J.: Scale-based difusive image filtering preserving boundary sharpness and fine structures. IEEE Transactions on Medical Imaging 20(11), 1140–1155 (2001)
9. Liu, G., Lin, Z., Yan, S., Sun, J., Yu, Y., Ma, Y.: Robust recovery of subspace structures by low-rank representation. IEEE Trans. on Pattern Analysis and Machine Intelligence 35, 171–184